Generation of oligodendroglial cells by direct lineage conversion

Nan Yang[1,2], **J. Bradley Zuchero**[3], **Henrik Ahlenius**[1,2], **Samuele Marro**[1,2], **Yi Han Ng**[1,2], **Thomas Vierbuchen**[1,2], **John S. Hawkins**[1,2], **Richard Geissler**[2], **Ben A. Barres**[3], and **Marius Wernig**[1,2]

[1]Institute for Stem Cell Biology and Regenerative Medicine, Stanford University School of Medicine, 265 Campus Drive, Stanford, CA 94305, USA

[2]Department of Pathology, Stanford University School of Medicine, 265 Campus Drive, Stanford, CA 94305, USA

[3]Departments of Neurobiology and Developmental Biology, Stanford University School of Medicine, 265 Campus Drive, Stanford, CA 94305, USA

Abstract

Transplantation of oligodendrocyte precursor cells (OPCs) is a promising potential therapeutic strategy for diseases affecting myelin. However, the derivation of engraftable OPCs from human pluripotent stem cells has proven difficult and primary OPCs are not readily available. Here we report the generation of induced OPCs (iOPCs) by direct lineage conversion. Forced expression of the three transcription factors Sox10, Olig2 and Zfp536 was sufficient to reprogram mouse and rat fibroblasts into iOPCs with morphologies and gene expression signatures resembling primary OPCs. More importantly, iOPCs gave rise to mature oligodendrocytes that could ensheath multiple host axons when co-cultured with primary dorsal root ganglion cells and formed myelin after transplantion into *shiverer* mice. We propose direct lineage reprogramming as a viable alternative approach for the generation of OPCs for use in disease modeling and regenerative medicine.

Oligodendrocyte precursor cells (OPCs) are resident progenitor cells distributed throughout the central nervous system. Their primary role is to differentiate into oligodendrocytes and ensheath axons with myelin during brain development and to remyelinate axons after brain damage. Myelination is a complex biological process involving axon recognition and attachment, membrane wrapping and compaction, and myelin maintenance[1, 2]. It is generally assumed that these tasks are accomplished by OPCs rather than by mature oligodendrocytes because transplantation studies in animal models have found that grafted OPCs readily myelinate whereas mature oligodendrocytes do not[2]. Therefore, OPCs have been identified as a promising cell population for therapeutic approaches in both

dysmyelinating and demyelinating diseases. In particular, genetic diseases affecting myelin, such as Pelizaeus-Merzbacher disease and other familial leukodystrophies, would be ideal candidates for cell-based therapies[3]. In addition, more prevalent conditions, such as spinal cord injury and multiple sclerosis, could benefit from OPC transplantation[2, 4, 5]. Notably, OPCs derived from the fetal brain or embryonic stem (ES) cells have been shown to remyelinate axons in rodent models of myelin diseases, in some cases with impressive therapeutic benefits[6-11]. Unfortunately, primary human tissue is limited and ES cell differentiation is slow and tedious[11-13].We therefore sought to determine whether OPCs can be generated by direct lineage conversion from readily-available somatic lineages such as fibroblasts.

Previously, we identified transcription factor combinations that mediate the rapid and efficient conversion of mouse fibroblasts directly into fully functional neuronal cells, which we called induced neuronal (iN) cells[14]. We and others further demonstrated the generation of iN cells from human fibroblasts[15]; a combination of our standard iN cell factors with additional subtype-specific factors allowed the generation of neuronal subtypes such as dopamine and motor neurons[16-18]; and, more recently, tripotent neural precursor cells were induced from mouse fibroblasts[19-24].

Here, we show that transcription factor-mediated reprogramming can also be applied to generate OPC-like cells. We found that forced expression of the three factors Sox10, Olig2, and Zfp536 converts rodent fibroblasts into iOPCs that express appropriate OPC markers, proliferate in OPC media conditions, differentiate into oligodendrocytes *in vitro* and myelinate host axons after transplantation into the dysmyelinated *shiverer* mouse brain.

RESULTS

A screen for OPC reprogramming factors

To identify candidate OPC reprogramming factors, we used data from detailed genome-wide expression studies and filtered the genes for transcription factors with greater expression in oligodendroglia compared to other neural lineages[25,26]. We selected 10 factors that participate in various stages of OPC specification and cause severe developmental oligodendroglia-related defects when mutated, including Ascl1, Gm98, Myt1, Nkx2.1, Nkx6.1, Nkx6.2, Olig1, Olig2, Sox10, and Zfp536. We utilized a well-characterized Proteolipid protein (Plp)::EGFP transgenic mouse strain, which expresses EGFP in both OPCs and mature oligodendrocytes, as a reporter for the presence of oligodendrocytic cells[27]. Mouse embryonic fibroblast (MEF) cultures were isolated from E14.5 embryonic limbs, a tissue source that we had previously shown to yield a fibroblast population essentially devoid of cells expressing markers of neurons, neural progenitors and neural crest stem cells (Ref 14 and Fig. 1a). The Plp::EGFP MEFs were transduced with a pool of 10 different lentiviruses containing the candidate genes and cultured in media known to support OPC proliferation. No EGFP expression was detected in cultures not infected or infected with control viruses based on fluorescence-microscopy or flow-cytometry analysis. In contrast, ~7 days after introducing the 10 factors, a small number of EGFP$^+$ cells appeared in the cultures. After another 14 days, cells were fixed and analyzed by immunofluorescence with O4 antibodies, known to specifically mark oligodendrocytes as

well as late-stage OPCs. This revealed the presence of Plp::EGFP[+]/O4^{+} cells with morphologies typical of oligodendrocytes (Fig. 1b **and** Supplementary Fig. 1). Thus, some combinations of the 10 candidate factors induced oligodendroglial properties in a fraction of the infected cells.

To identify the minimally required transcription factors for reprogramming towards the oligodendroglial lineage, we first determined whether any single factor was sufficient to generate EGFP^{+} cells. Among the 10 candidates, only Sox10 could activate the Plp::EGFP reporter, albeit in only a small fraction of infected cells (Fig. 1b). We then tested the reprogramming activity of Sox10 in combination with each of the remaining 9 candidate factors. Four factors (Nkx2.2, Nkx6.1, Olig2 and Zfp536) substantially increased the activity of Sox10 to generate EGFP^{+} cells (Fig. 1c). In a comprehensive process of systematic elimination, we determined that a combination of Sox10, Olig2 and Zfp536 was the minimal pool of factors sufficient to induce EGFP expression with the highest efficiency (Fig. 1d,e). We independently repeated these experiments using fluorescence activated cell sorting (FACS) to determine the fraction of EGFP^{+} cells after one week and observed similar results (Supplementary Fig. 2). Thus, we concluded that forced expression of the three factors Sox10, Olig2 and Zfp536 was the best of the combinations we tested to induce Plp::EGFP^{+} cells from MEFs.

Generation of induced OPCs from rat fibroblasts

Given the extensive characterization and well-established culture conditions for primary rat OPCs, we then tested whether the combination of Sox10, Olig2 and Zfp536 could convert rat fibroblasts into OPC-like cells (Fig. 2a). We observed large, proliferative clusters of cells with bipolar, OPC-like morphologies (Fig. 2b) that could be labeled with O4 antibodies 14 days after infection (Fig. 2c; Ref 26 and 28). These O4^{+} cells proliferated in response to platelet-derived growth factor (PDGF, a known OPC mitogen) as revealed by EdU incorporation (Supplementary Fig. 3). We also found some GFAP^{+} astrocytic cells but no Tuj1 or Map2-positive neurons 20 days after infection (Supplementary Fig. 4). After confirming the absence of O4^{+} cells in control rat fibroblasts (Supplementary Fig. 5), we used established immunopanning methods to purify the rat O4^{+} cells and used them for further characterizations in the rest of this study. Immunopanned O4^{+} cells exhibited typical OPC morphologies when placed in media containing PDGF and stained positive for three additional OPC markers, NG2, A2B5 and S100ß (Fig. 2d-g). PCR analysis of genomic DNA from immunopanned O4^{+} cells confirmed the integration of the three proviruses (Supplementary Fig. 6). Given that the fibroblast-derived O4^{+} cells proliferated in response to PDGF, exhibited typical morphologies and expressed key markers of OPCs, we called these cells "induced OPCs (iOPCs)". The observed GFAP^{+} cells could indicate the generation of an astrocyte-restricted progenitor or the spontaneous differentiation of a bipotent, glial-restricted progenitor. The absence of neurons may suggest that no intermediate tripotent neural progenitor cell was induced.

Next we characterized the reprogramming kinetics and efficiencies. As both fibroblasts and iOPCs are proliferative (Fig. 2h), the true cell conversion efficiency could not be determined. Instead, we assessed the iOPC yield, defined as the ratio of the number of O4-

immunopanned cells on day 20 after infection to the number of infected fibroblasts (see Methods). After seeding and infection of 2.4×10^5 fibroblasts/cm^2, ~25.9±4.9% of the fibroblasts expressed all three factors, and on average $6.8 \pm 1.7 \times 10^4$ O4$^+$ cells/cm^2 could be recovered 20 days after induction, resulting in a reprogramming yield of ~106.7% at this time point (Fig. 2i). The iOPC purity, defined as the ratio of O4-immunopanned cells to the total number of harvested cells on day 20, was on average 15.6±3.3% (Fig. 2j). We assume that the yield and purity values are both slight underestimates considering that cells strongly labeled by O4 antibody were not efficiently dissociated from the O4 antibody-coated panning plate. We note that the yield is a parameter dependent on reprogramming efficiency, cell death and proliferation and therefore the true reprogramming efficiency is almost certainly lower. Indeed, the yield of O4$^+$ cells was substantially lower at earlier time points, when the influence of cell proliferation may have been smaller (Fig. 2h). Moreover, the yield of functional iOPCs was even lower since the differentiation efficiency of O4$^+$ cells was ~25% that of primary neonatal OPCs (see below).

Global transcriptional remodeling in induced OPCs

We next compared the global gene expression pattern of rat iOPCs, fibroblasts, primary OPCs and their differentiated progeny by microarray analysis. A heatmap depicting all probe sets that were differentially expressed between any of the samples by at least 2-fold showed that the fibroblast-characteristic transcriptional program was globally reprogrammed towards that of the oligodendroglial lineage (Fig. 3a). Genes upregulated in iOPCs compared to fibroblasts were significantly enriched for GO terms associated with oligodendroglial biology (shown are all GO terms with a p value $<10^{-9}$). Conversely, fibroblast-characteristic genes with significantly enriched GO terms involving mesodermal cell functions were globally downregulated in iOPCs (Fig. 3a). Manual inspection of the gene clusters indicated that numerous genes known to be involved in progenitor self-renewal or oligodendroglial fate determination, such as Sox2, Sox6 and Nkx2.2, were strongly upregulated in iOPCs and OPCs compared to fibroblasts (Fig. 3a). The transcription levels of the fibroblast-specific genes *Col1a1, Col5a1* and *Thy1* were significantly downregulated (Fig. 3a). We confirmed the expression changes of these genes by quantitative RT-PCR (Fig. 3c, Supplementary Table 1). In agreement with these results, unsupervised hierarchical clustering analysis and Pearson's correlation analysis of the expression values of all differentially expressed genes showed that the transcriptional profile of iOPCs is much more similar to primary OPCs ($r^2=0.42$) than to fibroblasts ($r^2=0.15$) (Fig. 3b). Quantitative RT-PCR analysis demonstrated that the mRNA levels of some genes associated with the differentiation of OPCs, such as *Cdkn1c, Mbp, Mog* and *Plp1a*, are higher in iOPCs compared to primary OPCs to various degrees but lower than that of mature oligodendrocytes (Fig. 3c). However, the observed higher transcript levels of these differentiation-associated genes appeared to be insufficient to produce detectable protein as no MBP, PLP, CNP, or MOG-positive cells could be found in iOPC cultures based on immunofluorescence. In accordance with the quantitative RT-PCR results, Pearsons's correlation analysis showed a higher similarity of iOPCs to early differentiating OPCs than to undifferentiated OPCs (Fig. 3b).

Examination of the overall heatmap in Fig. 3a also suggested the induction of a set of genes in iOPCs that were not expressed in the oligodendroglial samples. Indeed, 31 probe sets representing 24 genes were found to be upregulated in iOPCs but not in any other samples (Supplementary Table 2). No coherent function could be assigned to this group of genes (Supplementary Table 3).

Induced OPCs differentiate into myelinating oligodendrocytes

To assess the functional properties of iOPCs, we first evaluated the differentiation potential of iOPCs *in vitro*. Upon PDGF withdrawal the immunopanned O4+ cells stopped dividing and differentiated into cells that expressed MBP and CNPase, and that exhibited mature oligodendrocytic morphologies (Fig. 4a and b). After three weeks of differentiation, 11.6±2.5% of the cells were MBP+. Given that OPCs can give rise to astrocytes *in vitro*, we also assessed GFAP and Nestin expression in differentiated iOPC cultures. GFAP+ (27.6±1.7%) and Nestin+ (29.0±5.0%) astrocytic cells were readily observed, however, no Tuj1 or Map2 positive neuronal cells were present (Fig. 4c,d **and** Supplementary Fig. 4).

We then evaluated the myelinogenic potential of the iOPCs *in vitro* using a co-culture system with dorsal root ganglion neurons (DRGs)[29]. Purified DRGs were allowed to extend dense beds of axons prior to plating O4-immunopanned iOPCs. Following 9 days of co-culture, iOPCs gave rise to MBP+ cells with complex oligodendrocytic morphology that were in close vicinity to the neurofilament+ axons (Fig. 4e). Many MBP+ cells extended multiple distinctive membrane extensions closely aligned with surrounding axons (Fig. 4e boxed cell). In the presence of DRGs, the differentiation efficiency of O4+ iOPCs into MBP+ oligodendrocytes slightly increased to 15.5±1.9% (Fig. 4f). This differentiation efficiency is ~25% of that of rat primary neonatal OPCs (B.Z., B.B., own observations).

To study the capacity of iOPCs to myelinate host axons *in vivo*, we transplanted the O4-immunopanned rat iOPCs into the *shiverer* mouse brains. These mice lack large portions of the *Mbp* gene and have dysmyelinated axons throughout the central nervous system[30, 31]. Thus, this transplantation model allows for unambiguous detection of graft-derived oligodendrocytes because any MBP signal must be derived from grafted cells. Purified iOPCs were injected bilaterally into the corpus callosum and cerebellum of neonatal mice (n=3). To maintain initial transgene expression, doxycycline, was added to the drinking water of nursing female mice for 3 weeks and grafted *shiverer* mice were sacrificed at 12 weeks of age, and their brains were cryosectioned and immunostained for MBP. In all 12 injection sites of the 3 grafted brains, small scattered groups of MPB+ cells forming tube-like structures were detected in the cortex, corpus callosum and white matter tract of the cerebellum (on average about 90-100 cells per injection site) (Fig. 5a,b). No similar structures were observed in non-transplanted *shiverer* brains following MBP staining. All MBP+ cells analyzed co-expressed Plp, the transmembrane proteolipid protein that is the predominant myelin protein present in the central but not peripheral nervous system (Fig. 5b). The MBP+ cells did not express Protein Zero (P0), the major structural protein of peripheral myelin or Peripherin (Fig. 5c **and** Supplementary Fig. 7). Confocal microscopy revealed that the MBP+ tube-like structures surrounded neurofilament+ axons, demonstrating oligodendroglial ensheathment of host axons by the transplanted iOPCs (Fig.

5d, e). Finally, we confirmed myelin formation of transplanted iOPCs on the ultrastructural level (Fig. 5f **and** Supplementary Fig. 8). These results demonstrate that fibroblast-derived iOPC can give rise to myelinating oligodendrocytes *in vivo*.

DISCUSSION

This paper demonstrates the principle that fibroblasts can be directly converted into induced OPCs by forced expression of just three defined transcription factors. Following the systematic evaluation of 10 candidate transcription factors we identified a minimally required combination of Sox10, Olig2, and Zfp536 that is sufficient to robustly induce OPC-like cells, termed iOPCs. These cells have the typical morphology of OPCs, express the relevant OPC markers O4, NG2 and A2B5, respond to PDGF signaling like OPCs and show a global transcriptional reprogramming towards an OPC-like profile. Notably, they give rise to mature oligodendrocytes that can myelinate host axons *in vivo*. This demonstrates that iOPCs are functional precursor cells and can execute the highly coordinated and complex cell biological processes involved in myelination, such as axon recognition and attachment, membrane wrapping and compaction. We observed small graft sizes, which was due to the extremely low short-term survival rate of freshly immunopanned cells. The detection of MBP^{+} cells in all grafted sites argues therefore for a remarkably robust *in vivo* differentiation capacity of iOPCs.

Several lines of evidence suggest that iOPCs are similar but not identical to primary OPCs. Compared to neonatal OPCs, the fibroblast-derived iOPCs have a lower efficiency of differentiation into mature oligodendrocytes and their gene expression profile is similar to, yet still distinct from that of primary OPCs, although the fibroblast-specific transcriptional network programs appear to be effectively downregulated. These transcriptional differences could be explained by several not mutually exclusive reasons. First, the iOPC cultures (as defined by O4 immunoreactivity) could represent a fairly heterogeneous population of fully and partially reprogrammed cells, similar to what was found in the first reports of induced pluripotent stem (iPS) cells[32-34]. However, while the transcriptional profile seems to be more similar to OPCs undergoing differentiation, the elevated mRNA levels of differentiation genes do not result in detectable protein or mature oligodendrocyte morphology, suggesting that they might not be functionally important. In addition, we observed a small group of aberrantly expressed genes unique to iOPCs. These might be direct or indirect targets of the reprogramming factors, which have documented roles in regulating other cell lineages (e.g. Sox10 in neural crest lineages, Olig2 in motor and ventral forebrain neurons). Future studies could address whether these fairly subtle differences may lead to detectable functional consequences.

Notably, we believe it to be highly unlikely that the described iOPCs are derived from contaminating neural crest stem cells or Schwann cell precursor cells. First, we have carefully dissected the tissue before fibroblast generation, minimizing contamination by neural crest progenitor cells. Second, we previously performed an extensive molecular characterization of these primary fibroblast cultures and found no evidence of neural crest or Schwann cell marker expression[14]. Third, we have demonstrated that iOPCs differentiate into myelinating cells, that are PLP[+], a marker that is specific to central oligodendrocytes,

and P0⁻, a specific marker of peripheral Schwann cells. Finally, we found that multiple host axons can be ensheathed by single engrafted cells, which is a typical feature of oligodendrocytes, whereas Schwann cells can only myelinate one axon per cell.

Given the strong clinical interest in OPCs for regenerative therapies, one of the most important next steps is to translate our findings to human fibroblasts. Based on our experience with iPS and iN cells, we predict that generation of human iOPCs is possible but may require additional reprogramming factors, such as other transcriptional regulators or microRNAs[15, 35-37]. Substantial optimization will likely be required to reliably generate large numbers of iOPCs form human cells that are functionally indistinguishable from OPCs of the human brain.

MATERIALS AND METHODS

Cell culture

Primary mouse and rat embryonic fibroblasts were isolated as previously described[14] and plated in MEF media (DMEM high glucose, calf serum, sodium pyruvate, non-essential amino acids, penicillin/streptomycin and β-mercaptoethanol). Before being used for experiments, primary fibroblast cells were passaged at least three times. Cortical OPCs were purified by sequential immunopanning and differentiated into OLs as described previously[29]. Basic media for OPC proliferation and differentiation: DMEM (Invitrogen) containing human transferrin (100 μg/ml), bovine serum albumin (100 μg/ml), putrescine (16 μg/ml), progesterone (60 ng/ml), sodium selenite (40 ng/ml), N-acetyl-L-cysteine (5 μg/ml), D-biotin (10 ng/ml), forskolin (4.2 μg/ml), bovine insulin (5 μg/ml) (all from Sigma), glutamine (2 mM), sodium pyruvate (1 mM), penicillin– streptomycin (100 U each) (all from Invitrogen), Trace Elements B (1×; Mediatech, Herndon, VA), and CNTF (10 ng/ml, Pepro Tech). Proliferation medium also contained OPC mitogens PDGF-AA (10 ng/ml) and NT-3 (1 ng/ml) (both from PeproTech); differentiation medium contained triiodothyronine (T3) (40 ng/ml; Sigma) without OPC mitogens. Mouse proliferation media also contained B27-supplement (Invitrogen).

Virus infections and efficiency calculation

Lentiviral Production and fibroblast infections were performed as described previously[14]. The transgenes were expressed from the tetO promoter. Cells were co-infected with a Ubiquitin promoter driving M2rtTA. Briefly, primary fibroblasts were plated on poly-D-lysine coated plates and infected with concentrated lentiviral particles and polybrene (8 μg/μl) in fresh MEF medium. Viral medium was removed after 16–24 h and replaced with MEF medium containing doxycycline (2 μg/μl). After 24 h, medium was changed to proliferation medium containing doxycycline (2 μg/μl). All chemicals were purchased from Sigma-Aldrich if not otherwise specified. 48 h after addition of doxycycline, rat fibroblasts were fixed with 4% paraformaldehyde and immunofluorescence stainings were performed using antibodies specific to Sox10 or Olig2. Nuclei were visualized by DAPI staining. On average ~63% of Sox10 or Olig2 positive cells were detected. Because of the lack of Zpf536 antibody, we had to estimate the percentage of Zfp536 positive cells and assume that the

number is similar to that of Sox10 or Olig2 positive cells. Therefore, we estimated that the fraction of cells that express all three factors is around 26%.

Immunofluorescence, RT-PCR, and Flow Cytometry

Immunofluorecence stainings were performed as previously described [15]. The following antibodies were used for our analyses mouse anti-O4 and -MOG hybridoma supernatants, mouse anti-CNP1 (Millipore, 1:1000), rat anti- MBP (Abcam ab7349, 1:1000), rabbit anti-neurofilament (Sigma, 1:1000), rabbit anti-NG2 (a gift from Dr. Bill Stallcup, 1:400), mouse anti-Plp (Abcam, 1:1000), mouse anti-A2B5 (Millipore, 1:50). For EdU labeling, 10 μM EdU (Invitrogen) was added into media and incubated for 6 h. EdU incorporation was detected using Click-iT® EdU Alexa Fluor® 555 Imaging Kit (Invitrogen) following the manufacturer's instructions. EGFP cells were analyzed and sorted on a FACS Aria II, and flow cytometry data were analyzed using FlowJo Software (Tree Star, Inc.). For RT–PCR analysis, RNA was isolated using an RNAqueous Kit (Applied Biosystems) following the manufacturer's instructions, treated with DNase (Applied Biosystems) and reverse-transcribed with Superscript III (Invitrogen).

iOPC Immunopanning

Purification of iOPCs away from fibroblasts was performed by O4 immunopanning[26], with the following modifications. iOPC/fibroblast cultures were treated with trypsin (Sigma) to release cells and DNaseI (Worthington) to prevent cell clumping. Following inactivation of trypsin with 30% fetal calf serum, cells were pelleted and resuspended in panning buffer containing 0.02% BSA, insulin (5μg/mL), and DNaseI. Cells were passed through a Nitex filter (20 μm pore size, Sefar America) and incubated on O4-coated panning plates for 30 minutes at room temperature. Following stringent washing with DPBS to remove cells that were not tightly adhered to the plate (i.e. fibroblasts), iOPCs were either released with trypsin or lysed directly on the plate for RNA extraction.

Microarray Analysis

The following cell populations were profiled: O4-immunopanned iOPCs from rat embryonic fibroblasts 20 days after infection, freshly isolated OPCs from the neonatal rat neocortex, 3 and 6 days differentiated primary rat OPCs that were expanded in proliferation media (see above) for 24h after isolation before switching into differentiation medium, and rat embryonic fibroblasts. Cells were collected by immunopanning and total RNA was extracted using RNeasy kit (Qiagen) hybridized to Rat Genome 230 2.0 Affymetrix array per manufacturer's instruction. Gene expression levels were defined using standard Affymetrix protocol. Hierarchical clustering with centroid linkage clustering was performed [38]. All fold changes were expressed in $\log_2$ values. Analysis was performed using Partek® software, version 6.4 © 2008 Partek Inc., St. Louis, MO, USA. The complete microarray data set is available at GEO under the accession number GSE40421.

Cell Quantifications

When calculating the efficiency of Plp::EGFP positive cell induction, we counted the number of EGFP^{+} cells in at least 15 randomly selected 20× visual fields on a Zeiss Axio Observer microscope as previously described[15]. Data are presented as mean±s.d.

Myelinating co-culture

Myelinating co-cultures were generated as described[29]. Dorsal route ganglion neurons were grown on glass coverslips coated with rat collagen and mouse laminin (Cultrex), with alternating feedings containing antimitotic (5-*Fluoro*-2′-deoxyuridine, 10μM) for at least one week prior to seeding iOPCs in DMEM-sato (above) plus NS21[39] and T3 (20ng/mL). Co-cultures were fixed after 9 days and immunostained for MBP and neurofilament (axons) as above. Under these conditions MBP immunoreactivity was never observed in the absence of iOPCs.

Transplantation, histology and electron microscopy

On postnatal day 1, after hypothermia-induced anesthesia, homozygous shiverer × rag2 immunodeficient pups, were injected bilaterally with 100,000 purified rat iOPCs targeted to the corpus callosum and cerebellum, respectively. At 12.5 wk after transplantation, mice were transcardially perfused with saline followed by 4% paraformaldehyde fixation buffer. After over night post-fixation, brains were cryoprotected in 30% sucrose and cut into 40-μm sagittal sections. Free-floating sections were washed in PBS, treated with antigenretrieval solution (Dako) at 80 °C for 30 min, blocked in in 0.25% Triton-X-100 PBS with 5% CCS, and stained overnight using rabbit anti-Neurofilament 1, rabbit anti-PLP and mouse anti-MBP. Following washes, sections were incubated with secondary antibodies for 2 h at room temperature, washed again, mounted on glass slides, and coverslipped.

To prepare the sections for electron microscopy, for preembedding immunofluorescence, 60 μm vibratome sections were permeabilized with 0.25% Triton-X-100 PBS, incubated with the antibody to MBP followed by the Alexa Fluor 555 donkey anti-mouse secondary antibody (Invitrogen). Regions containing grafted were microdissected, photographed and postfixed overnight in glutaraldehyde, photodocumented, dehydrated in graded ethanol series, and embedded in Epon (Epoxy-Embedding kit; Fluka, Buchs, Switzerland). Semi-thin (1 μm) sections were stained with toluidine blue to visualize the details of the materials. Fiber bundles myelinated by transplanted cells were then localized on semi-thin sections at the light microscope using several landmarks (Supplementary Fig. 8a,b). Ultrathin sections (80-90 nm) were cut for regions of interest, transferred to a mesh copper grid, stained with uranyl acetate and lead citrate, and viewed on a transmission electron microscope. MBP[+] fiber bundles were again unambiguously identified (Supplementary Fig. 8c). Despite the slightly decreased preservation of the ultrastructure caused by immunofluorescence staining procedure, this analysis allowed the detection of the presence of axons that are wrapped with multiple, densely organized sheets of myelin originating from the transplanted cells.

Supplementary Material

Refer to Web version on PubMed Central for supplementary material.

ACKNOWLEDGEMENTS

REFERENCES

1. Potter GB, Rowitch DH, Petryniak MA. Myelin restoration: progress and prospects for human cell replacement therapies. Arch Immunol Ther Exp (Warsz). 2011; 59:179–193. [PubMed: 21461592]

2. Franklin RJ, Ffrench-Constant C. Remyelination in the CNS: from biology to therapy. Nat Rev Neurosci. 2008; 9:839–855. [PubMed: 18931697]

3. Goldman SA. Progenitor cell-based treatment of the pediatric myelin disorders. Arch Neurol. 2011; 68:848–856. [PubMed: 21403006]

4. Cummings BJ, et al. Human neural stem cells differentiate and promote locomotor recovery in spinal cord-injured mice. Proc Natl Acad Sci U S A. 2005; 102:14069–14074. [PubMed: 16172374]

5. Franklin RJ, Ffrench-Constant C. Stem cell treatments and multiple sclerosis. BMJ. 2010; 340:c1387. [PubMed: 20223864]

6. Brustle O, et al. Embryonic stem cell-derived glial precursors: a source of myelinating transplants. Science. 1999; 285:754–756. [PubMed: 10427001]

7. Learish RD, Brustle O, Zhang SC, Duncan ID. Intraventricular transplantation of oligodendrocyte progenitors into a fetal myelin mutant results in widespread formation of myelin. Ann Neurol. 1999; 46:716–722. [PubMed: 10553988]

8. Sim FJ, et al. CD140a identifies a population of highly myelinogenic, migration-competent and efficiently engrafting human oligodendrocyte progenitor cells. Nat Biotechnol. 2011; 29:934–941. [PubMed: 21947029]

9. Windrem MS, et al. Fetal and adult human oligodendrocyte progenitor cell isolates myelinate the congenitally dysmyelinated brain. Nat Med. 2004; 10:93–97. [PubMed: 14702638]

10. Windrem MS, et al. Neonatal chimerization with human glial progenitor cells can both remyelinate and rescue the otherwise lethally hypomyelinated shiverer mouse. Cell Stem Cell. 2008; 2:553–565. [PubMed: 18522848]

11. Wang S, et al. Human iPSC-Derived Oligodendrocyte Progenitor Cells Can Myelinate and Rescue a Mouse Model of Congenital Hypomyelination. Cell Stem Cell. 2013; 12:252–264. [PubMed: 23395447]

12. Keirstead HS, et al. Human embryonic stem cell-derived oligodendrocyte progenitor cell transplants remyelinate and restore locomotion after spinal cord injury. J Neurosci. 2005; 25:4694–4705. [PubMed: 15888645]

13. Najm FJ, et al. Rapid and robust generation of functional oligodendrocyte progenitor cells from epiblast stem cells. Nat Methods. 2011; 8:957–962. [PubMed: 21946668]

14. Vierbuchen T, et al. Direct conversion of fibroblasts to functional neurons by defined factors. Nature. 2010; 463:1035–1041. [PubMed: 20107439]

15. Pang ZP, et al. Induction of human neuronal cells by defined transcription factors. Nature. 2011; 476:220–223. [PubMed: 21617644]

16. Caiazzo M, et al. Direct generation of functional dopaminergic neurons from mouse and human fibroblasts. Nature. 2011; 476:224–227. [PubMed: 21725324]

17. Pfisterer U, et al. Direct conversion of human fibroblasts to dopaminergic neurons. Proc Natl Acad Sci U S A. 2011; 108:10343–10348. [PubMed: 21646515]

18. Son EY, et al. Conversion of mouse and human fibroblasts into functional spinal motor neurons. Cell Stem Cell. 2011; 9:205–218. [PubMed: 21852222]

19. Kim J, et al. Direct reprogramming of mouse fibroblasts to neural progenitors. Proc Natl Acad Sci U S A. 2011; 108:7838–7843. [PubMed: 21521790]

20. Lujan E, Chanda S, Ahlenius H, Sudhof TC, Wernig M. Direct conversion of mouse fibroblasts to self-renewing, tripotent neural precursor cells. Proc Natl Acad Sci U S A. 2012; 109:2527–2532. [PubMed: 22308465]

21. Thier M, et al. Direct conversion of fibroblasts into stably expandable neural stem cells. Cell Stem Cell. 2012; 10:473–479. [PubMed: 22445518]

22. Han DW, et al. Direct reprogramming of fibroblasts into neural stem cells by defined factors. Cell Stem Cell. 2012; 10:465–472. [PubMed: 22445517]

23. Matsui T, et al. Neural stem cells directly differentiated from partially reprogrammed fibroblasts rapidly acquire gliogenic competency. Stem Cells. 2012; 30:1109–1119. [PubMed: 22467474]

24. Ring KL, et al. Direct reprogramming of mouse and human fibroblasts into multipotent neural stem cells with a single factor. Cell Stem Cell. 2012; 11:100–109. [PubMed: 22683203]

25. Cahoy JD, et al. A transcriptome database for astrocytes, neurons, and oligodendrocytes: a new resource for understanding brain development and function. J Neurosci. 2008; 28:264–278. [PubMed: 18171944]

26. Dugas JC, Tai YC, Speed TP, Ngai J, Barres BA. Functional genomic analysis of oligodendrocyte differentiation. J Neurosci. 2006; 26:10967–10983. [PubMed: 17065439]

27. Mallon BS, Shick HE, Kidd GJ, Macklin WB. Proteolipid promoter activity distinguishes two populations of NG2-positive cells throughout neonatal cortical development. J Neurosci. 2002; 22:876–885. [PubMed: 11826117]

28. Barres BA, et al. Cell death and control of cell survival in the oligodendrocyte lineage. Cell. 1992; 70:31–46. [PubMed: 1623522]

29. Chan JR, et al. NGF controls axonal receptivity to myelination by Schwann cells or oligodendrocytes. Neuron. 2004; 43:183–191. [PubMed: 15260955]

30. Roach A, Boylan K, Horvath S, Prusiner SB, Hood LE. Characterization of cloned cDNA representing rat myelin basic protein: absence of expression in brain of shiverer mutant mice. Cell. 1983; 34:799–806. [PubMed: 6194889]

31. Scolding N. MYELIN BIOLOGY AND ITS DISORDERS: TWO-VOLUME SET Edited by Robert A. Lazzarini 2004. San Diego: Elsevier Academic Press Price£ 340.00. ISBN 0-12-439510-4. Brain. 2004; 127:2144–2147.

32. Meissner A, Wernig M, Jaenisch R. Direct reprogramming of genetically unmodified fibroblasts into pluripotent stem cells. Nat Biotechnol. 2007; 25:1177–1181. [PubMed: 17724450]

33. Takahashi K, Yamanaka S. Induction of pluripotent stem cells from mouse embryonic and adult fibroblast cultures by defined factors. Cell. 2006; 126:663–676. [PubMed: 16904174]

34. Wernig M, et al. A drug-inducible transgenic system for direct reprogramming of multiple somatic cell types. Nat Biotechnol. 2008; 26:916–924. [PubMed: 18594521]

35. Yu J, et al. Induced pluripotent stem cell lines derived from human somatic cells. Science. 2007; 318:1917–1920. [PubMed: 18029452]

36. Takahashi K, et al. Induction of pluripotent stem cells from adult human fibroblasts by defined factors. Cell. 2007; 131:861–872. [PubMed: 18035408]

37. Yoo AS, et al. MicroRNA-mediated conversion of human fibroblasts to neurons. Nature. 2011; 476:228–231. [PubMed: 21753754]

38. Eisen MB, Spellman PT, Brown PO, Botstein D. Cluster analysis and display of genome-wide expression patterns. Proc Natl Acad Sci U S A. 1998; 95:14863–14868. [PubMed: 9843981]

39. Chen Y, et al. NS21: re-defined and modified supplement B27 for neuronal cultures. J Neurosci Methods. 2008; 171:239–247. [PubMed: 18471889]
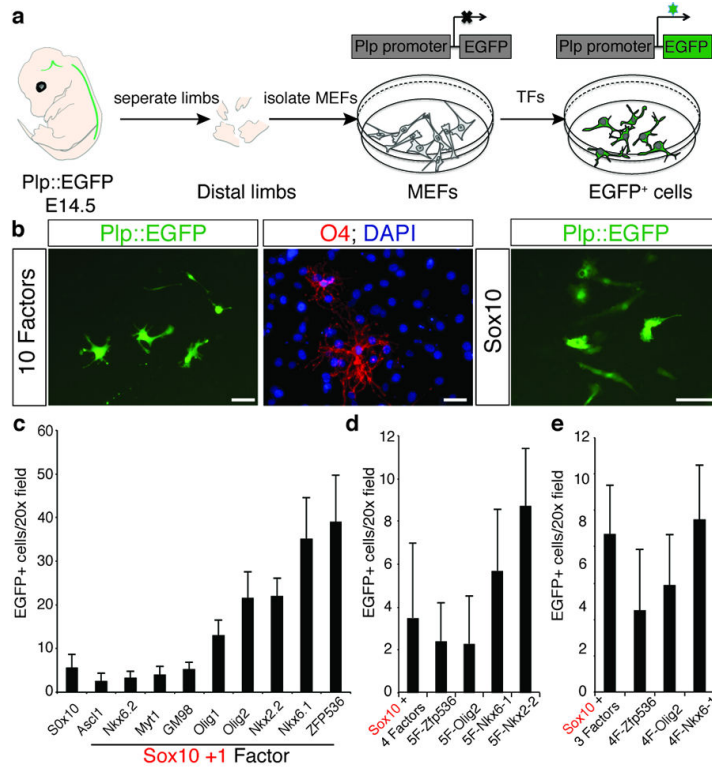
Figure 1. Identification of candidate factors for the generation of iOPCs
(**a**) Schematic representation of the strategy to test candidate OPC-inducing factors. (**b**) Plp::EGFP+ cells and O4-labeled cells derived from MEFs 3 weeks after infection with the 10-factor pool. Ectopic expression of Sox10 alone is sufficient to induce Plp::EGFP positive cells. (**c, d, e**) Quantification of Plp::EGFP+ cells with indicated factor combinations 3 weeks after transgene induction. Shown are average numbers of EGFP+ cells per 20× visual field from at least 15 randomly picked fields. Data are presented as mean ± SD. Scale bars, 50 μm (**b**).
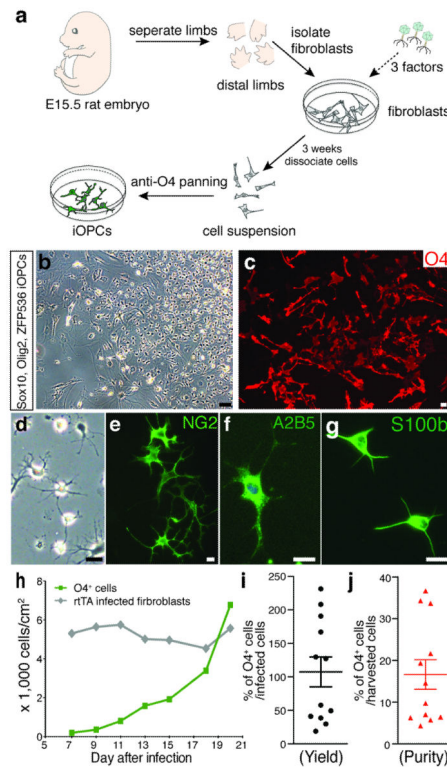
Figure 2. Induction of OPC-like cells from rat fibroblasts

(**a**) Schematic of the experimental setup and strategy to derive and isolate iOPCs from rat embryonic fibroblasts. (**b**) Phase contrast image of iOPCs derived from rat fibroblasts by a combination of 3 factors (Sox10, Olig2 and Zfp536) three weeks after infection. (**c**) iOPCs with immature morphology can be labeled with O4 antibodies 3 weeks after infection. (**d**) Phase contrast image of O4-immunopanned iOPCs in proliferation media. (**e-g**) O4$^+$ cells can be labeled with additional OPC markers including NG2 (e), A2B5 (f), S100β (g) 3 weeks after infection. (**h**) FACS analysis revealed an initial slow and later exponential increase of O4$^+$ cells during reprogramming whereas the total number of rtTA virus infected fibroblasts cultured in OPC expansion media did not change over time. (**i**) The reprogramming yield was determined by the ratio of O4-immunopanned cells/cm^2 20 days after induction and the total number of fibroblasts that ectopically express all three reprogramming factors 48h after infection. For both (i) and (k) shown are individual data points, averages and SEM. (**k**) The purity of iOPCs on day 20 was determined by the ratio of recovered O4$^+$ cells after immunopanning and the total number of harvested cells before immunopanning. Scale bars, 100 μm (**b**), 50 μm (**c, d**), 20 μm (**e, f, g**).
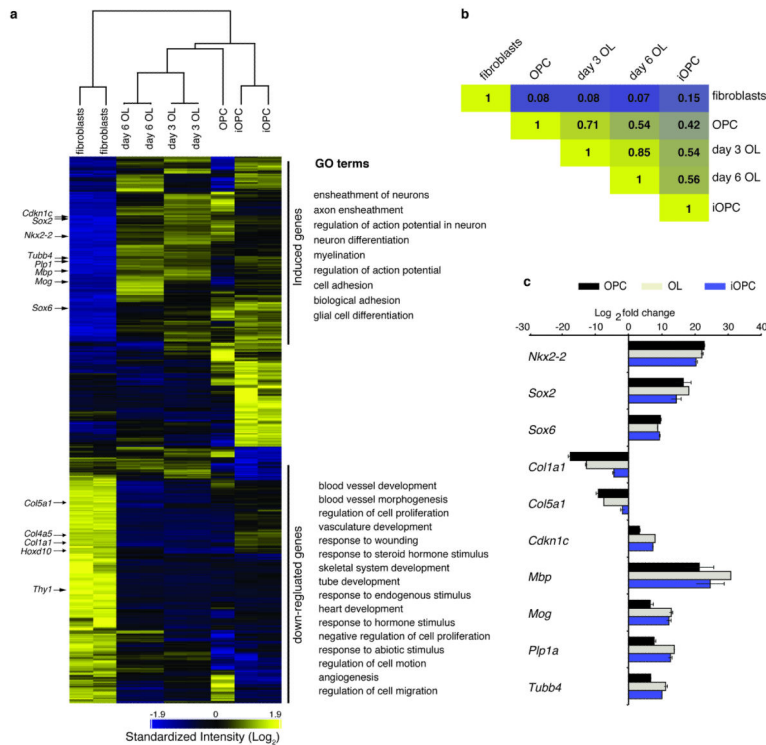
Figure 3. Global transcriptional reprogramming of iOPCs

(**a**) Heatmap of microarray data illustrating differentially expressed genes among iOPCs, fibroblasts, OPCs, and OPCs differentiated for 3 or 6 days (day 3 oligodendrocytes (OLs), day 6 OLs). Shown are 5,765 probe sets selected on fold change ±2 in iOPCs vs. fibroblasts. Expression levels are shown as mean centered $\log_2$ values. Yellow indicates up-regulated genes whereas blue indicates down-regulated genes. The scale extends from 1.988- to 15.691-fold over mean (−2 to +2 in $\log_2$ space) as indicated at the bottom. Hierarchical clustering among all the samples is presented as array tree. The position of representative fibroblast and OPC genes is indicated by arrows. Significantly enriched Gene ontology (GO) terms ($p<10^{-9}$) of induced and repressed gene clusters in iOPCs after reprogramming are shown on the right side of the heatmap. (**b**) Pearson's correlation analyses of all differentially expressed genes among fibroblasts, OPC, day3 OLs, day6 OLs and iOPCs. R^2 values are indicated on a corresponding heatmap. (**c**) qRT-PCR analysis of the expression levels of characteristic OPC, fibroblast and oligodendrocyte marker genes in fibroblasts, iOPCs, OPCs and differentiated OPCs (OL). Data are presented as $\log_2$ fold change between indicated cell types and fibroblasts.
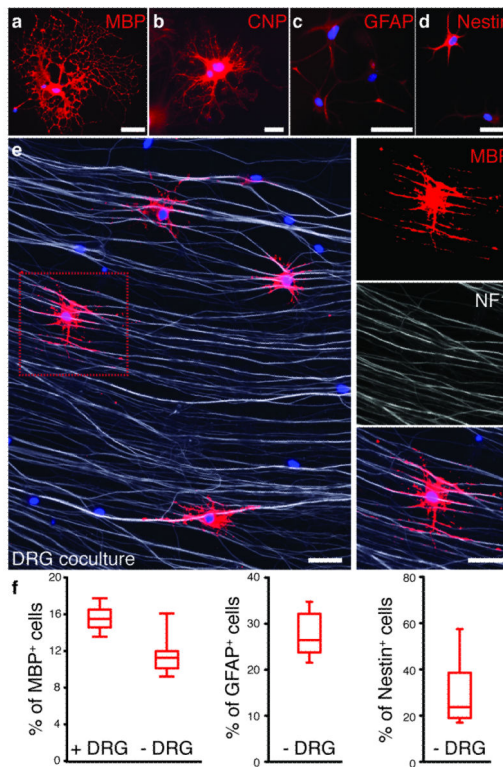
Figure 4. Differentiation potential of fibroblasts-derived iOPCs *in vitro*
Three weeks after culture in differentiation medium, iOPCs adopt mature oligodendrocyte morphologies and express MBP (**a**) and CNP (**b**). GFAP (**c**) and Nestin (**d**) expressing cells were also detected. (**e**) When iOPCs were co-cultured with pre-established dorsal root ganglion neurons (DRGs), mature oligodendrocytes were identified by MBP immunofluorescence (red). Myelinating iOPC-derived oligodendrocytes extended multiple distinctive smooth tubes, which were aligned with axons marked by neurofilament (NF) staining (grey). The right panels represent zoomed images of the boxed area showing MBP, NF staining. (**f**) Quantification of MBP, GFAP, and Nestin-positive cells 3 weeks after differentiation of iOPCs with or without DRGs. Scale bars, 50 μm (**a-d**), 20 μm (**e**).
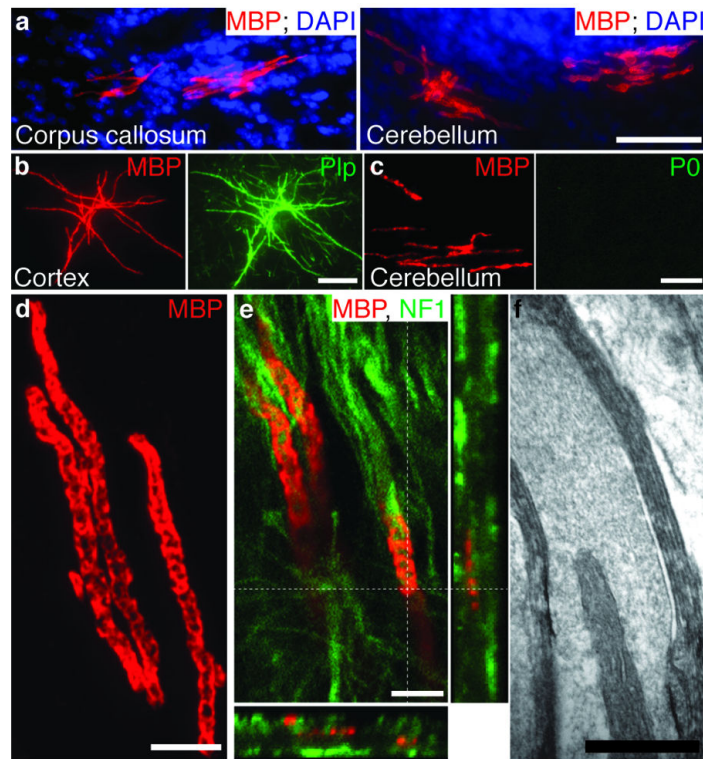
Figure 5. Fibroblasts-derived iOPC cells are myelinogenic *in vivo*
(**a**) iOPCs purified by immunopanning were injected into early perinatal *Mbp^shi/shi* mice and brains were analyzed 12 weeks later. MBP+ cells with typical mature oligodendrocyte morphology were detected in all injection sites analyzed (n=3 brains, 4 injection sites/brain). Nuclei were counterstained with DAPI (blue). (**b, c**) All engrafted MBP+ cells express the additional oligodendrocyte marker Plp but not P0. (**d**) Confocal projection image showing the MBP+ tube-like structures in the *Mbp^shi/shi* mouse brain. (**e**) Single-focal plane image showing the close association of nerve fibers revealed by neurofilament immunofluorescence (green) and MBP+ oligodendrocyte membrane wraps (red). (**f**) Electron microscope image showing dense myelin sheaths formed by engrafted iOPCs in the *Mbp^shi/shi* mouse brain. Scale bars, 20 μm (**a**), 50 μm (**b,c**), 10 μm (**d,e**), 500 nm (**f**).